PHYSICAL REVIEW C **84**, 061601(R) (2011)

Systematics of fusion probability in "hot" fusion reactions

Ning Wang,[1] Junlong Tian,[2,*] and Werner Scheid[3]

[1]*Department of Physics, Guangxi Normal University, Guilin 541004, People's Republic of China*

[2]*School of Physics and Electrical Engineering, Anyang Normal University, Anyang 455002, People's Republic of China*

[3]*Institut für Theoretische Physik der Universität, D-35392 Giessen, Germany*

(Received 25 November 2011; published 27 December 2011)

The fusion probability in "hot" fusion reactions leading to the synthesis of superheavy nuclei is investigated systematically. The quasifission barrier influences the formation of the superheavy nucleus around the "island of stability" in addition to the shell correction. Based on the quasifission barrier height obtained with the Skyrme energy-density functional, we propose an analytical expression for the description of the fusion probability, with which the measured evaporation residual cross sections can be reproduced acceptably well. Simultaneously, some special fusion reactions for synthesizing new elements 119 and 120 are studied. The predicted evaporation residual cross sections for $^{50}\mathrm{Ti} + {}^{249}\mathrm{Bk}$ are ∼10–150 fb at energies around the entrance-channel Coulomb barrier. For the fusion reactions synthesizing element 120 with projectiles $^{54}\mathrm{Cr}$ and $^{58}\mathrm{Fe}$, the cross sections fall to a few femtobarns, which seems beyond the limit of the available facilities.

DOI: 10.1103/PhysRevC.84.061601 PACS number(s): 25.70.Jj, 27.90.+b, 24.10.−i, 21.10.Dr

Synthesis of superheavy nuclei (SHN) through fusion reactions is a field of very intense studies in recent decades [1–17]. Up to now, the superheavy elements $Z = 107 - 118$ have already been synthesized [1–6] through "cold" fusion reactions that use lead or bismuth targets with appropriate projectiles following the emission of one or two neutrons from a "cold" compound system, or "hot" fusion reactions that use actinide targets from uranium to californium with beams of $^{48}\mathrm{Ca}$ following the evaporation of three to five neutrons from a "hot" system. The reaction $^{50}\mathrm{Ti} + {}^{249}\mathrm{Cf}$ for producing element 120 is currently being studied in GSI without a result up to now [18]. Besides the experiments, both the structure of SHN and the mechanism of fusion reactions are also being intensively investigated theoretically. On one hand, the precise calculation of the masses and the shell correction of SHN, which plays a key role in determining the fission barrier and the center of the "island of stability" for SHN, is of great importance. Recently, Liu *et al.* [19] proposed an improved macroscopic-microscopic mass model (also called the Weizsäcker-Skyrme mass model) with a rms error of 336 keV with respect to the 2149 known masses and 248 keV to the measured α-decay energies of 46 superheavy nuclei, with which they found that the SHN with the largest shell corrections are located at approximately $Z = 116$–120 and $N = 178$ rather than at $N = 184$. It is found that the difference of the calculated evaporation residual cross sections for reactions leading to element 120 reaches two orders of magnitude by adopting two different mass tables for SHN [15]. It is therefore interesting to investigate the production cross sections of SHN in fusion reactions by using the Weizsäcker-Skyrme mass model.

On the other hand, the fusion probability of heavy nuclei and superheavy nuclei should be systematically investigated for testing the models and for giving reliable predictions of fusion reactions leading to new superheavy elements. Theoretical support for these very time-consuming and extremely expensive experiments is vital for choosing the optimum target-projectile-energy combinations and for the estimation of cross sections. In the practical calculation of the evaporation residue cross section, the reaction process leading to the synthesis of SHN can be divided into three steps. First, the projectile is captured by the target and a dinuclear system is formed, which then evolves into the compound nucleus, and, finally, the compound nucleus loses its excitation energy mainly by the emission of particles and γ rays and goes to its ground state. The simplified version of the evaporation residue cross section is given by [14,20]

$$\sigma_{\mathrm{ER}}(E_{\mathrm{c.m.}}) = \sigma_{\mathrm{cap}}(E_{\mathrm{c.m.}})P_{\mathrm{CN}}(E_{\mathrm{c.m.}})W_{\mathrm{sur}}(E_{\mathrm{c.m.}}). \quad (1)$$

Here, σ_{cap}, P_{CN}, and W_{sur} denote the capture cross section of the colliding nuclei overcoming the Coulomb barrier, the probability of the compound nucleus formation (i.e., the fusion probability) after the capture, and the survival probability of the excited compound nucleus, respectively. The most unclear part may be the value of P_{CN} which is usually calculated by different models for the dynamics [10,12,13] based on the potential energy surface of the reaction system or by empirical formulas [12,21]. In Refs. [20,22–24], the methods for the calculation of σ_{cap} and W_{sur} are well established in general, with the Skyrme energy-density functional and an empirical barrier distribution for describing the capture cross sections and with the HIVAP code [25–27] for describing the survival probability of the compound nuclei. Based on previous work [20], the fusion probability in reactions leading to SHN will be further systematically investigated in this Rapid Communication by applying the Weizsäcker-Skyrme mass model for describing the masses of SHN.

We first investigate the relation between the fission barrier height, the quasifission barrier height, and the evaporation residual cross sections for some fusion reactions leading to SHN. The fission barrier height B_{f} of a nucleus can be approximately estimated by the shell correction $\Delta E^{\mathrm{shell}}$ and

*tianjunlong@gmail.com

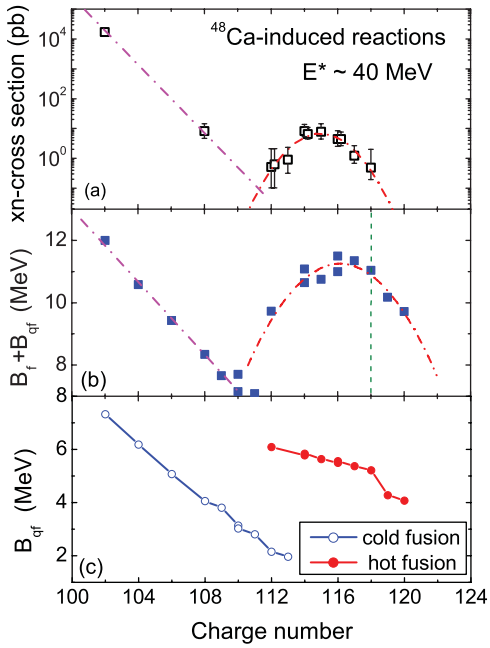

FIG. 1. (Color online) (a) Measured evaporation residual cross sections of some ^{48}Ca-induced reactions. The data are extracted from a figure in Oganessian's talk [28]. (b) Sum of fission barrier height and quasifission barrier height for some fusion reactions leading to the synthesis of superheavy nuclei as a function of the charge number of SHN. The dotted-dashed curves are to guide the eyes. The vertical dashed line shows the position of $Z = 118$ and the squares on its right-hand side denote the results for ^{50}Ti + ^{249}Bk and ^{50}Ti + ^{249}Cf. (c) Quasifission barrier height for these reactions. The open and solid circles denote the results for "cold" and "hot" fusion reactions, respectively.

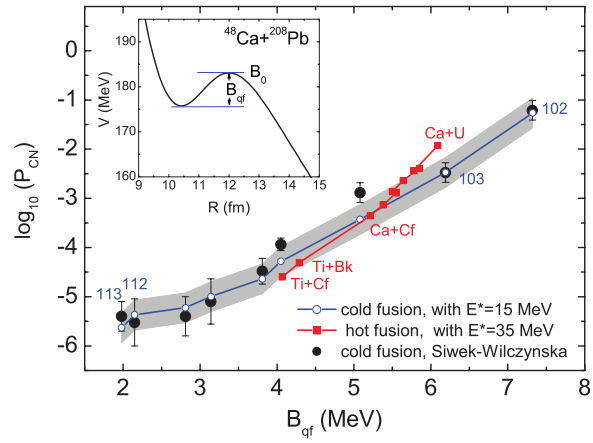

FIG. 2. (Color online) Fusion probability in reactions leading to superheavy nuclei as a function of quasifission barrier height. The open circles and the solid circles denote the calculated results for "cold" fusion reactions with excitation energy $E^* = 15$ MeV and the extracted fusion probability in Ref. [14] for the same reactions, respectively. The solid squares denote the results for "hot" fusion reactions with $E^* = 35$ MeV. Subfigure: Calculated entrance-channel potential for ^{48}Ca + ^{208}Pb. B_{qf} and B_0 denote the depth of the pocket and the height of the Coulomb barrier, respectively.

the macroscopic fission barrier B_f^{Mac} of the nucleus [20], i.e.,

$$B_f \approx B_f^{Mac} + \Delta E^{Shell} = B_f^{Mac} + (E_{exp} - E_{LD}). \quad (2)$$

Here, E_{exp} and E_{LD} denote the measured binding energy and the liquid drop energy of the nucleus (positive values), respectively. Figure 1(a) shows the measured evaporation residual cross sections for some ^{48}Ca-induced reactions as a function of the charge number of the compound nucleus. The data are extracted from a figure in Oganessian's talk [28], and these data are also shown in Ref. [29]. At $Z \approx 114$–116 there exists a peak for the cross sections, which seems to be evidence of the center of the "island of stability" for superheavy nuclei being located at $Z \leqslant 120$. Figure 1(b) shows the sum of the fission barrier height and the quasifission barrier height for some fusion reactions leading to the synthesis of SHN. Here, the quasifission barrier height B_{qf} is defined as the depth of the capture pocket in the entrance-channel potential (see the subfigure in Fig. 2), which is calculated by using the Skyrme energy-density functional [30] together with the extended Thomas-Fermi approximation including all terms up to the second order in the spatial derivatives (ETF2) as mentioned in Ref. [22]. For calculating the shell corrections in Fig. 1(b), the obtained binding energies and the corresponding liquid-drop energies E_{LD} of the SHN in Ref. [19] are adopted. One sees that the dependence of $B_f + B_{qf}$ on the charge number is very similar to the dependence of the evaporation residual cross sections on the charge number. The peak at $Z \approx 116$ in Fig. 1(b) comes from the contributions of the shell correction and the quasifission barrier height. The quasifission barrier height decreases linearly with the charge number of the compound nucleus [see Fig. 1(c)], and the largest shell corrections are located at approximately $Z = 116$–120 according to the Weizsäcker-Skyrme mass model. The sum of the shell correction ΔE^{Shell} and the quasifission barrier height results in the peak at $Z \approx 114$–116 of the evaporation residual cross sections. Figure 1 indicates that the quasifission barrier influences the formation of the superheavy nuclei around the known "island of stability" in addition to the shell correction. For very asymmetric fusion reactions leading to intermediate and heavy nuclei rather than the SHN, the quasifission barrier is relatively high. With the increase of the charge number of the projectile or target nuclei in the fusion reactions leading to the synthesis of SHN, the quasifission barrier height decreases gradually.

It is known that the fission barrier height strongly influences the survival probability of superheavy nuclei. In addition, one expects that the fusion probability increases with increasing quasifission barrier height and the incident energies in the reactions leading to the SHN [16]. To consider the contribution of the quasifission barrier, we propose an analytical formula for description of the fusion probability P_{CN},

$$P_{CN}(E^*) = \frac{1}{C} \exp(3B_{qf} + 0.3E^*), \quad (3)$$

where $E^* = E_{c.m.} + Q$ denotes the excitation energy of the compound nucleus (in MeV). In addition, we introduce a truncation for the value of P_{CN}, i.e., P_{CN} should not be larger than 1. The parameters in Eq. (3) with $C = \exp(50|\eta|)$ are

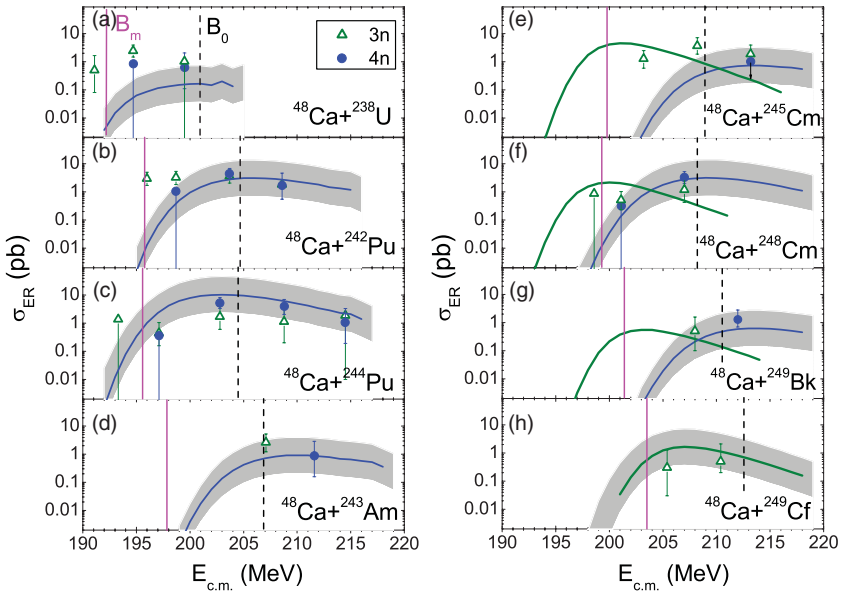

FIG. 3. (Color online) Evaporation residual cross sections for some "hot" fusion reactions. The data are taken from Refs. [6,32]. The dashed and solid lines denote the entrance-channel Coulomb barrier height B_0 under the sudden approximation for the densities and the mean barrier height B_m, respectively. The green (light gray) and blue (dark gray) curves denote the corresponding calculation results for the $3n$ and $4n$ channels with $C = \exp(50|\eta|)$, respectively. The shades show the uncertainty of the calculated σ_{ER} for the $4n$ channel [except (h) in which the shades are for the $3n$ channel].

determined by fitting the measured evaporation residual cross sections of ^{48}Ca + ^{248}Cm and ^{48}Ca + ^{249}Cf. Here, $\eta = (A_1 - A_2)/(A_1 + A_2)$ denotes the mass asymmetry of the reaction system. For ^{48}Ca-induced "hot" fusion reactions leading to SHN, $|\eta| \approx 0.67$. The calculation for the capture cross sections and the survival probability of compound nucleus are the same as those in Ref. [20] except that the masses of unknown nuclei are given by the Weizsäcker-Skyrme mass model [19] rather than by the finite range droplet model (FRDM) [31]. Figure 2 shows the fusion probability in reactions leading to SHN as a function of the quasifission barrier height B_{qf}. The solid squares denote the results for "hot" fusion reactions with an excitation energy of $E^* = 35$ MeV. The open and solid circles denote the calculated results for "cold" fusion reactions with $E^* = 15$ MeV and the extracted fusion probability in Ref. [14] for the same reactions, respectively. Here the parameter C is slightly different for the "cold" fusion reactions, which will be discussed later. The corresponding evaporation residual cross sections for these reactions will be shown in Figs. 3–5. The shades show the estimated uncertainty of the calculated fusion probability with Eq. (3). With a decrease of the quasifission barrier height, the fusion probability decreases exponentially. The obtained fusion probabilities in this paper and those in Ref. [14] are very close to each other for the "cold" fusion reactions. In addition, it seems that the obtained fusion probability for the "cold" fusion reaction and that for the "hot" fusion reaction are comparable when their quasifission barrier heights are close to each other.

Figure 3 shows the evaporation residual cross sections for some "hot" fusion reactions. The open triangles and solid circles denote the experimental data for the $3n$ and $4n$ channels, respectively. The green (light gray) and blue (dark gray) curves denote the corresponding calculated results. The dashed and solid lines denote the entrance-channel Coulomb barrier height B_0 from the Skyrme energy-density functional and the mean barrier height $B_m \approx 0.956B_0$ according to the empirical barrier distribution [22], respectively. The shades show the corresponding uncertainty of this approach due to the systematic errors in the calculation of σ_{cap}, W_{sur}, and P_{CN}, which is approximately a factor of 4.4 for σ_{ER} at energies above the mean barrier height B_m. The estimated uncertainties [20] for σ_{cap}, W_{sur}, and P_{CN} are approximately factors of 1.18, 1.85, and 2.0 at $E_{c.m.} > B_m$, respectively. We would like to state that the parameters in Eq. (3) are determined just by the reactions ^{48}Ca + ^{248}Cm and ^{48}Ca + ^{249}Cf. With the same parameters we find that the experimental data of other "hot" fusion reactions can also be reproduced reasonably well.

To further test the model, the "cold" fusion reactions leading to SHN are also investigated systematically. In Fig. 4, we show the evaporation residual cross sections for some "cold" fusion reactions. The solid squares and open circles denote the experimental data for the $1n$ and $2n$ channels, respectively. The blue (dark gray) and green (light gray) solid curves denote the corresponding calculated results. Here, we slightly change the parameter $C = \exp(47|\eta|)$, considering the differences between the "cold " fusion reactions and the "hot" fusion reactions. Carrying out the same calculations as for the"hot" fusion reactions, we can roughly reproduce the measured evaporation residual cross sections for the "cold" fusion reactions. The larger uncertainty for the "cold" fusion reactions at sub-barrier energies is due to the factor g in the barrier distribution function for calculating the capture cross sections [20].

The above calculations give us great confidence for investigating the evaporation residual cross sections of fusion reactions leading to the synthesis of new elements. Figure 5 shows the predicted evaporation residual cross sections for the reactions $^{50}_{22}$Ti + $^{249}_{97}$Bk, $^{50}_{22}$Ti + $^{249}_{98}$Cf, $^{54}_{24}$Cr + $^{248}_{96}$Cm, and $^{58}_{26}$Fe + $^{244}_{94}$Pu leading to the synthesis of the elements 119 and 120. The solid and dashed curves denote the results for the $3n$ and $4n$ channels, respectively. For the reaction ^{50}Ti + ^{249} Bk $\rightarrow$ ^{295}119 + $4n$, the obtained evaporation residual cross sections σ_{ER} are ~10–150 fb at incident energies around the entrance-channel Coulomb barrier B_0. For the reactions synthesizing element 120, the calculated σ_{ER} are smaller than those for element 119, and the σ_{ER} falls to a few femtobarns for the latter

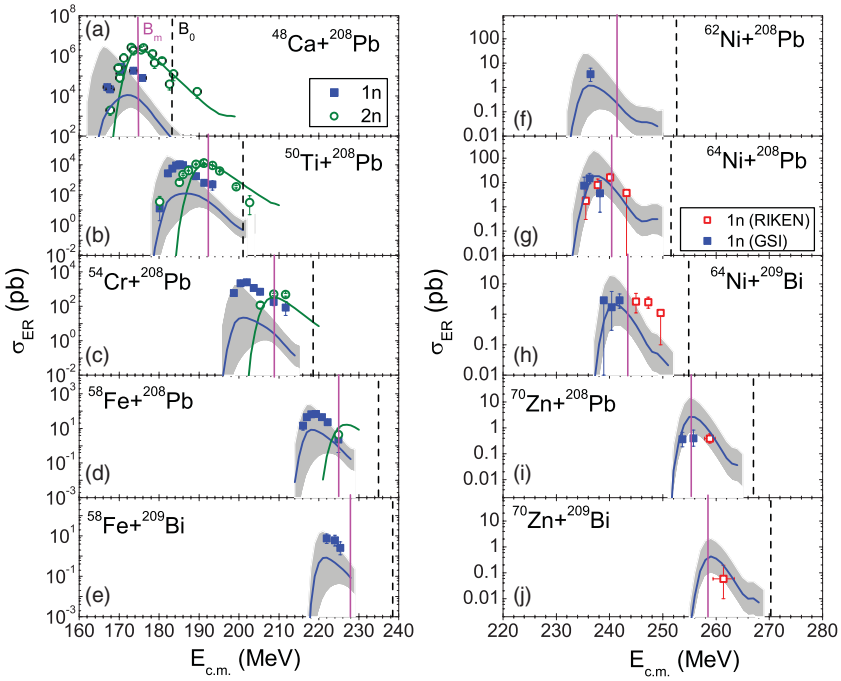

FIG. 4. (Color online) The same as Fig. 3, but for some "cold" fusion reactions. Here, we adopt $C = \exp(47|\eta|)$ in the calculations. The data are taken from Ref. [32]. The shades show the uncertainty of the calculated σ_{ER} for the 1n channel.

two reactions ^{54}Cr + ^{248}Cm and ^{58}Fe + ^{244}Pu. Here, we would like to state that the parameter C in Eq. (3) for the description of the fusion probability depends on the parameter sets for calculating the survival probability of superheavy nuclei. If one takes a different liquid-drop formula for calculating the fission barrier, the parameter C must be readjusted. Adopting different formulas for describing the liquid-drop energies [19,33] and the binding energies of yet unmeasured nuclei [19,31] (the parameter C is readjusted to fit the measured σ_{ER} of "hot" fusion reactions), we find that the calculated evaporation residual cross sections for the four reactions leading to the elements 119 and 120 are close to the corresponding results in Fig. 5, with deviations which are smaller than the uncertainty of this approach. To compare with the results from other models, we list in Table I the calculated optimal evaporation residual cross sections from four different models for the four reactions mentioned in Fig. 5. One sees that, for ^{50}Ti + ^{249}Bk and ^{50}Ti + ^{249}Cf, the results from Ref. [10] with the fusion-by-diffusion model and Ref. [34] with the dinuclear system model are in the same order of magnitude (hundreds of fb), while the results from Ref. [12] and those in this paper are in the same order of magnitude (tens of fb). All models in Table I predict that the optimal evaporation residual cross sections for ^{50}Ti + ^{249}Cf $\rightarrow$ $^{299-xn}$120 are smaller than those for ^{50}Ti + ^{249}Bk $\rightarrow$ $^{299-xn}$119.

In summary, the entrance-channel Coulomb barrier determines the capture cross sections, the quasifission barrier due to the pocket in the entrance-channel potential influences

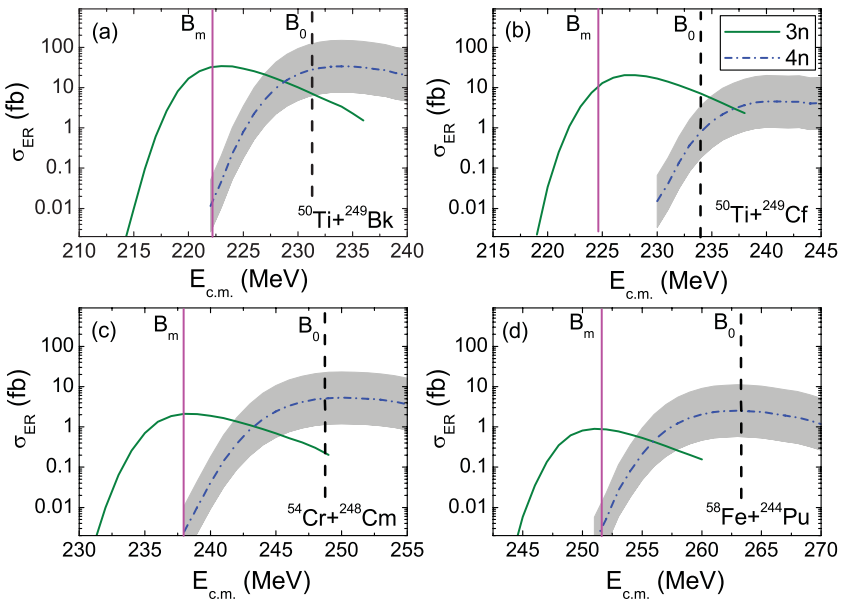

FIG. 5. (Color online) The same as Fig. 3 but for fusion reactions leading to the synthesis of elements 119 and 120 (in femtobarn). The green solid and blue dotted-dashed curves denote the predicted results for the $3n$ and $4n$ channels with $C = \exp(50|\eta|)$, respectively.

TABLE I. The predicted optimal evaporation residual cross section (in femtobarn) for four reactions leading to elements 119 and 120.

Reference	^{50}Ti+^{249}Bk	^{50}Ti+^{249}Cf	^{54}Cr+^{248}Cm	^{58}Fe+^{244}Pu
Liu [10]	∼600	∼100		
Nan Wang [34]	∼1000	∼200	∼40	∼30
Zagrebaev [12]	∼50	∼40	∼20	∼5
This work	∼35	∼20	∼5	∼3

the fusion probability, and the fission barrier is related to the survival probability, and all play an important role for a reliable calculation of the evaporation residual cross sections in fusion reactions leading to the synthesis of SHN. Of course the dynamics of the fusion process and the zero-point motion for fission process [35,36] also influence the cross sections significantly, but it is beyond the scope of this work. Based on the previously established methods for the calculation of capture cross sections and the survival probability, we further proposed an analytical formula with only three fixed parameters for a systematic description of the fusion probability in reactions leading to SHN. With this formula the measured evaporation residual cross sections for the "hot" fusion reactions can be reproduced reasonably well. The predicted evaporation residual cross sections σ_{ER} for the reaction $^{50}\mathrm{Ti} + {}^{249}\mathrm{Bk}$ are ∼10–150 fb at incident energies around the entrance-channel Coulomb barrier, and the predicted σ_{ER} for the reactions $^{54}\mathrm{Cr} + {}^{248}\mathrm{Cm}$ and $^{58}\mathrm{Fe} + {}^{244}\mathrm{Pu}$ falls to a few femtobarns, which seems beyond the limit of the available facilities.

We thank Shan-Gui Zhou for a careful reading of the manuscript, and Jing-Dong Bao for a useful discussion. This work was supported by National Natural Science Foundation of China, No. 10875031, No. 10847004, No. 11005003, and No. 10979024.

[1] S. Hofmann and G. Münzenberg, Rev. Mod. Phys. **72**, 733 (2000).
[2] Yu. Ts. Oganessian *et al.*, Phys. Rev. C **62**, 041604(R) (2000).
[3] Yu. Ts. Oganessian *et al.*, Phys. Rev. C **69**, 021601(R) (2004).
[4] K. Morita *et al.*, J. Phys. Soc. Jpn. **73**, 2593 (2004).
[5] Yu. Ts. Oganessian *et al.*, Phys. Rev. C **74**, 044602 (2006).
[6] Yu. Ts. Oganessian *et al.*, Phys. Rev. Lett. **104**, 142502 (2010).
[7] S. Cwiok, P. H. Heenen, and W. Nazarewicz, Nature (London) **433**, 705 (2005).
[8] A. Sobiczewski and K. Pomorski, Prog. Part. Nucl. Phys. **58**, 292 (2007).
[9] C. Shen, D. Boilley, Q. Li, J. Shen, and Y. Abe, Phys. Rev. C **83**, 054620 (2011).
[10] Z. H. Liu and J. D. Bao, Phys. Rev. C **84**, 031602(R) (2011).
[11] R. K. Gupta, M. Manhas, G. Münzenberg, and W. Greiner, Phys. Rev. C **72**, 014607 (2005).
[12] V. Zagrebaev and W. Greiner, Phys. Rev. C **78**, 034610 (2008).
[13] G. G. Adamian, N. V. Antonenko, and V. V. Sargsyan, Phys. Rev. C **79**, 054608 (2009).
[14] K. Siwek-Wilczyńska, I. Skwira-Chalot, and J. Wilczyński, Int. J. Mod. Phys. E **16**, 483 (2007).
[15] A. K. Nasirov, G. Mandaglio, G. Giardina, A. Sobiczewski, and A. I. Muminov, Phys. Rev. C **84**, 044612 (2011).
[16] M. Huang, Z. Gan, X. Zhou, J. Li, and W. Scheid, Phys. Rev. C **82**, 044614 (2010).
[17] B. N. Lu, E. G. Zhao, and S. G. Zhou, arXiv:1110.6769.
[18] Ch. E. Düllmann, "News from TASCA," talk given at the 10th Workshop on Recoil Separator for Superheavy Element Chemistry, 2011, GSI (unpublished).
[19] M. Liu, N. Wang, Y. Deng, and X. Wu, Phys. Rev. C **84**, 014333 (2011).
[20] N. Wang, K. Zhao, W. Scheid, and X. Wu, Phys. Rev. C **77**, 014603 (2008); [http://www.imqmd.com/wangning/hivap2.rar].
[21] W. Loveland, Phys. Rev. C **76**, 014612 (2007).
[22] M. Liu, N. Wang, Z. Li, X. Wu, and E. Zhao, Nucl. Phys. A **768**, 80 (2006).
[23] N. Wang, X. Wu, Z. Li, M. Liu, and W. Scheid, Phys. Rev. C **74**, 044604 (2006).
[24] N. Wang, M. Liu, and Y. Yang, Sci. China G **52**, 1554 (2009).
[25] W. Reisdorf, Z. Phys. A **300**, 227 (1981).
[26] W. Reisdorf *et al.*, Nucl. Phys. A **444**, 154 (1985).
[27] W. Reisdorf and M. Schädel, Z. Phys. A **343**, 47 (1992).
[28] Y. Oganessian, "SHE in JINR," talk given at the 109th Session of the JINR Scientific Council, 2010, Dubna (unpublished).
[29] A. Popeko, "Plans of Superheavy Elements Investigations in FLNR," talk given at the Annual NuSTAR Meeting, 2010, GSI (unpublished).
[30] J. Bartel, Ph. Quentin, M. Brack, C. Guet, and H. B. Hakansson, Nucl. Phys. A **386**, 79 (1982).
[31] P. Möller, J. R. Nix, W. D. Myers, and W. J. Swiatecki, At. Data Nucl. Data Tables **59**, 185 (1995).
[32] J. Tian, N. Wang, and Z. Li, Chin. Phys. Lett. **24**, 905 (2007), and references therein.
[33] W. D. Myers and W. J. Swiatecki, Ark. Fys. **36**, 342 (1967).
[34] Nan Wang (private communication).
[35] U. Mosel and W. Greiner, Z. Phys. **222**, 261 (1969).
[36] R. Smolańczuk, J. Skalski, and A. Sobiczewski, Phys. Rev. C **52**, 1871 (1995).